Supplementary information for

Episodic Creep Events on the San Andreas Fault Caused by Pore Pressure Variations

Mostafa Khoshmanesh[1]*

Manoochehr Shirzaei[1]

[1]School of Earth and Space Exploration, Arizona State University, Tempe, AZ, USA

***e-mail: mkhm@asu.edu**

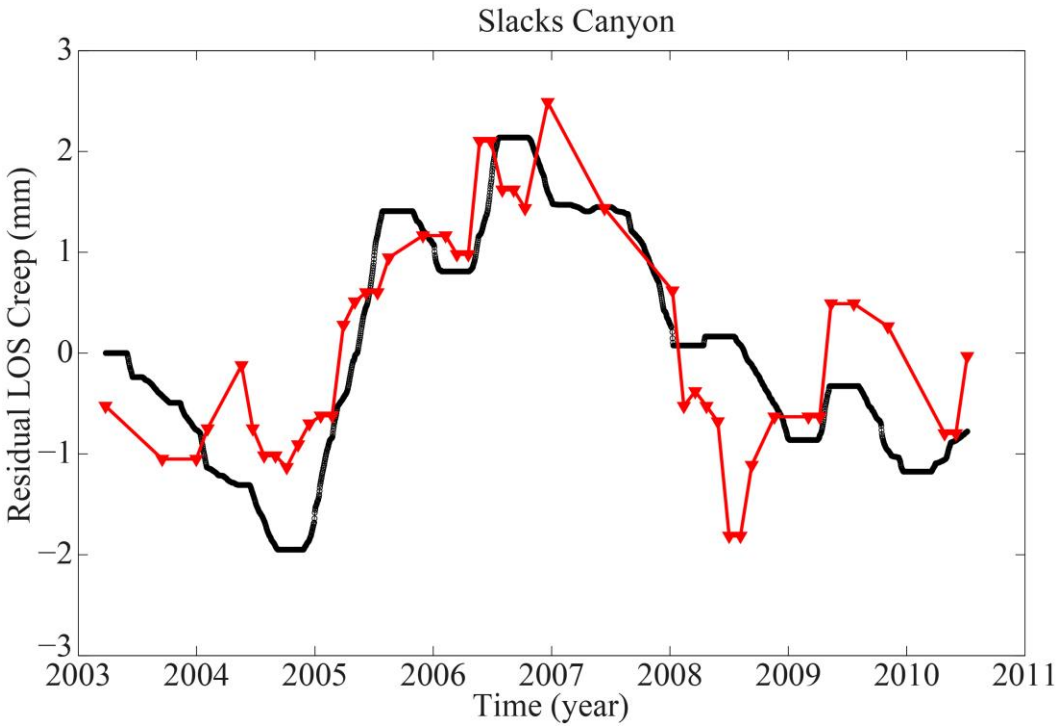

Supplementary Fig. 1| Comparison between InSAR time series and creepmeter measurements for Slacks Canyon station, after removing a long-term trend from both data sets. We additionally have applied a 6-month boxcar smoothing filter to both data sets.

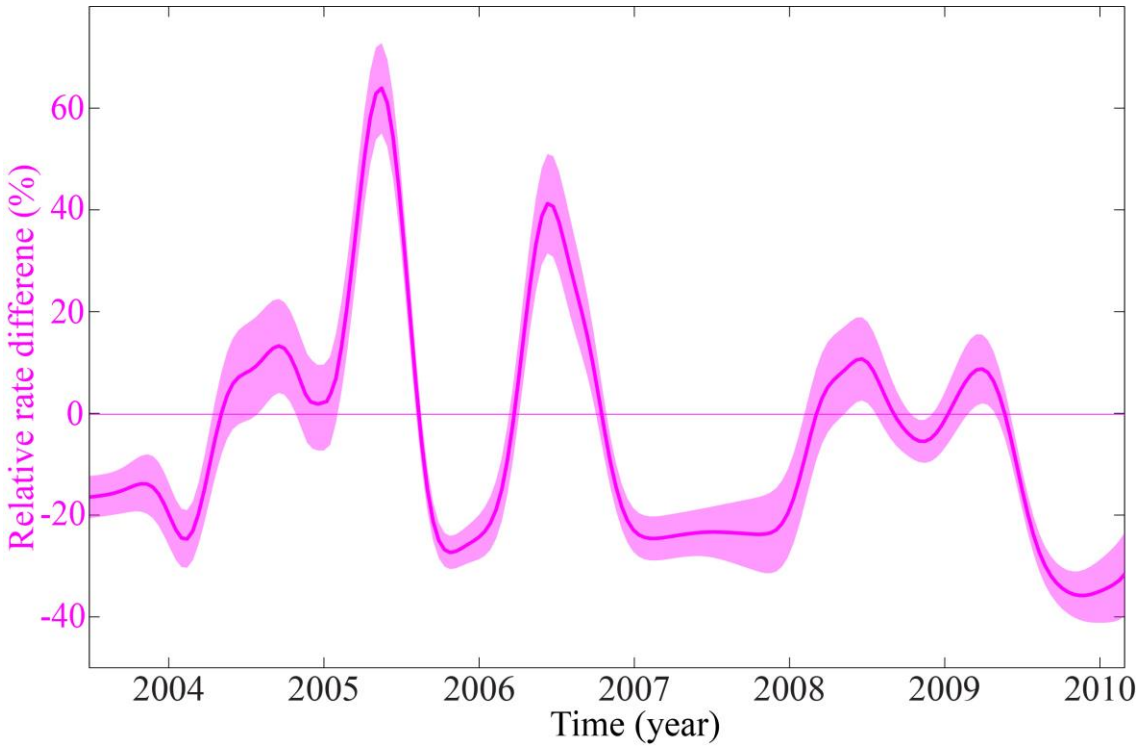

Supplementary Fig. 2| Spatially averaged LOS creep rate difference and its one-sigma uncertainty shown with the magenta shaded area. The time series is smoothed using a Gaussian smoothing filter of size 6 months.

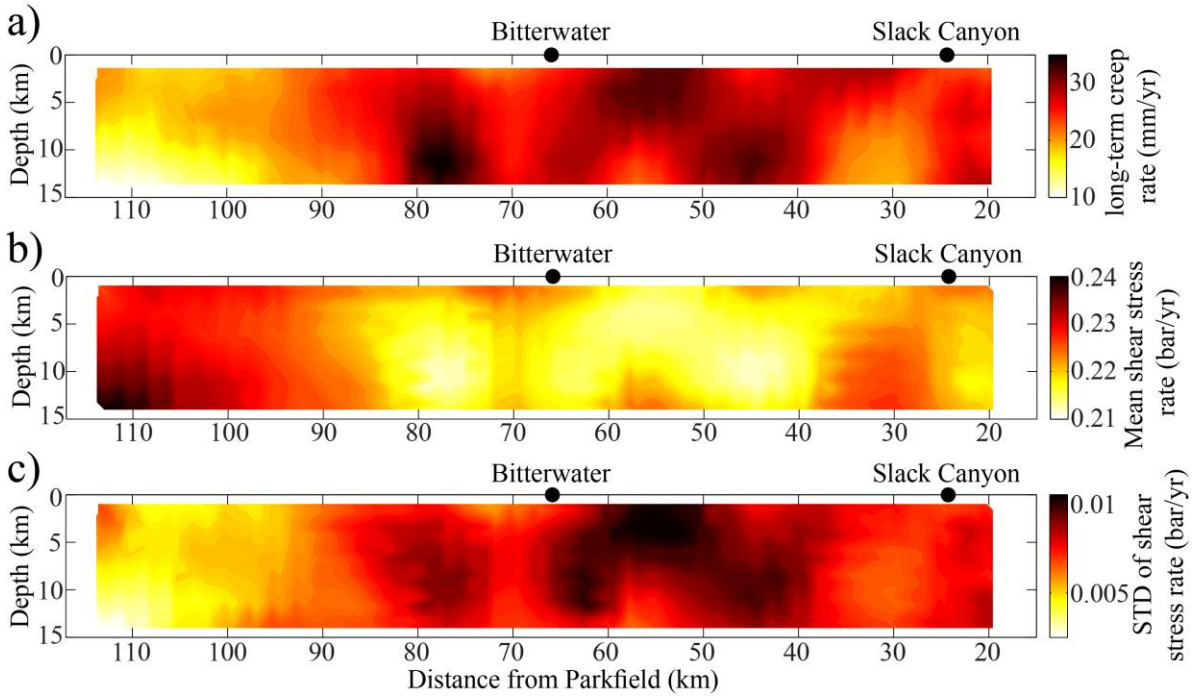

Supplementary Fig. 3| Spatial distribution of long-term modeled creep rate from Khoshmanesh et al. (2015) in mm/yr (**a**), temporal average (**b**) and standard deviation (**c**) of shear stress rate along the CSAF in bar/yr.

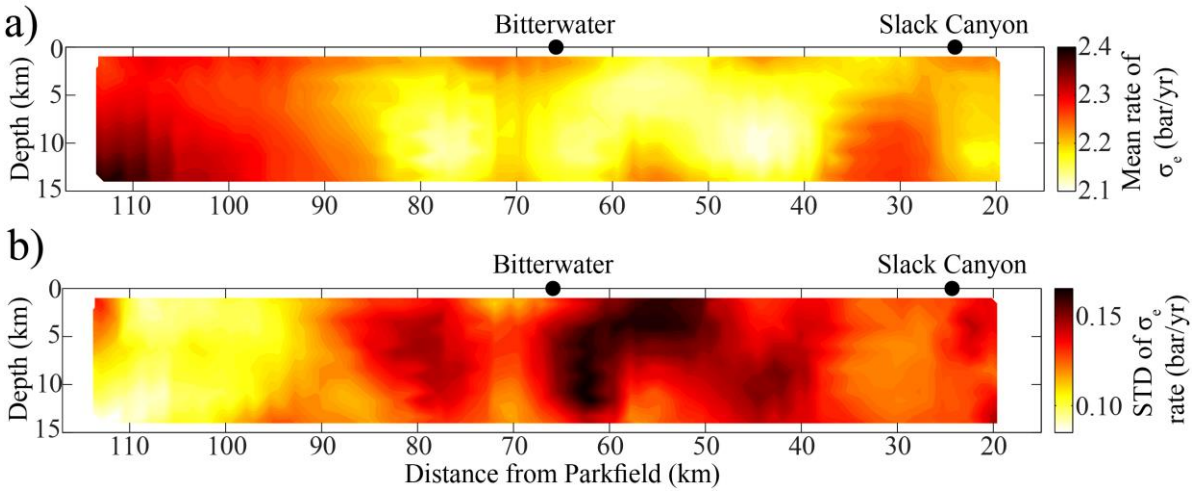

Supplementary Fig. 4| Spatial distribution of temporal mean (**a**) and standard deviation (**b**) of effective normal stressing rate along the CSAF in bar/yr.

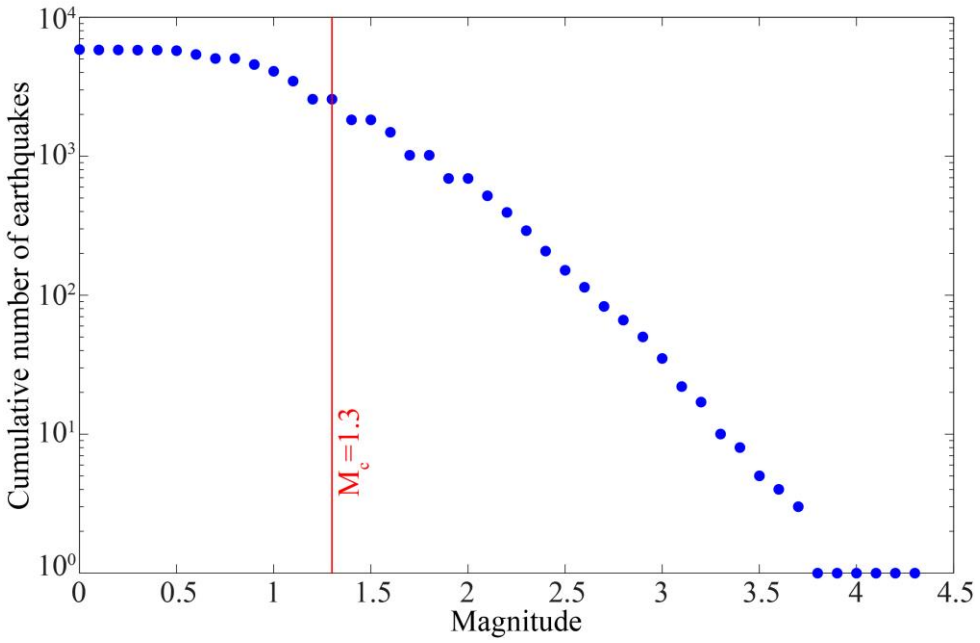

Supplementary Fig. 5| Frequency-Magnitude distribution of all the earthquakes used for *b*-value time series analysis.

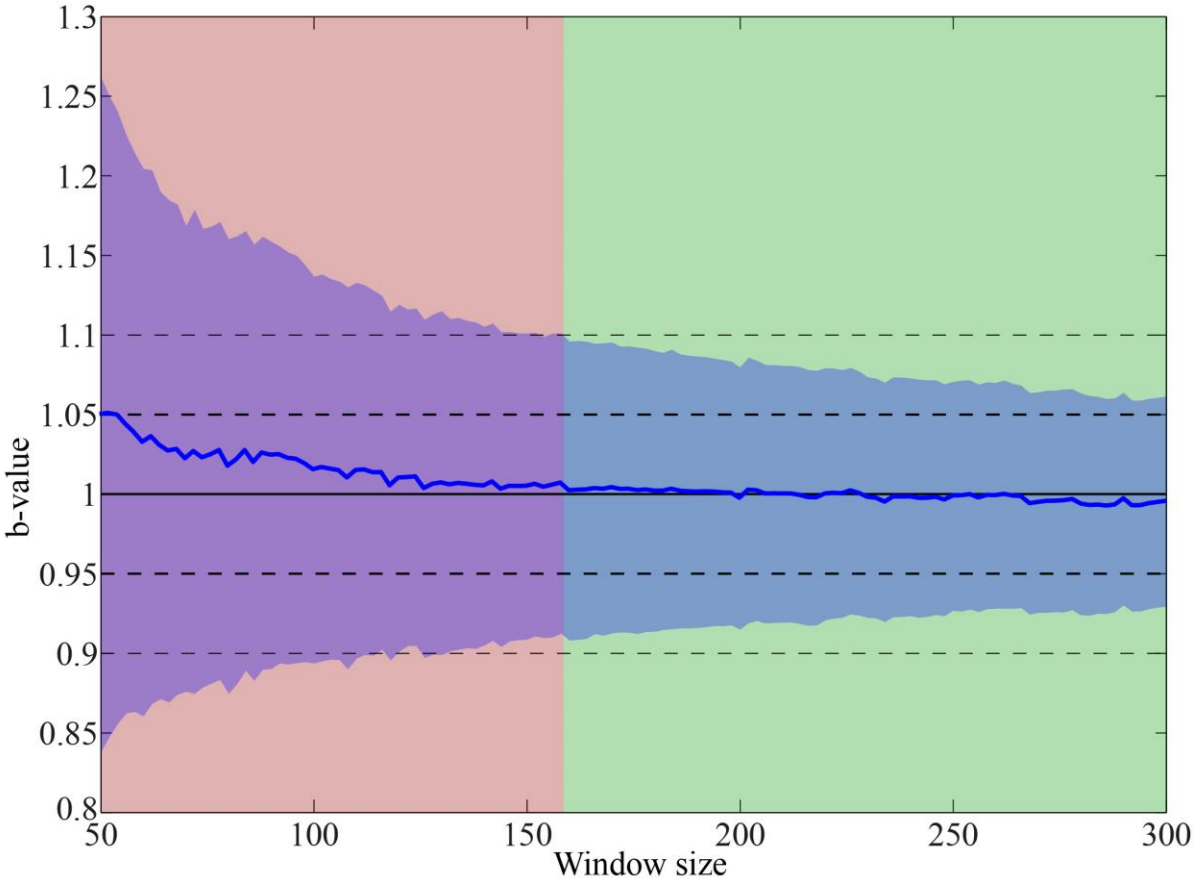

Supplementary Fig. 6| Optimization of the window size using the Monte Carlo search algorithm. The blue curve shows the estimated mean *b*-value for each window size across 1000 random simulations. The shaded blue area shows the standard deviation of estimated *b*-value. For each sample size, the *b*-value and the corresponding standard deviation associated with the time step with maximum uncertainty across all simulations is shown. The true *b*-value of b_0=1 is shown by the horizontal solid black line. The two thick and thin dashed lines indicate the acceptable range of accuracy and precision, respectively. The green and red shaded area highlights the range of acceptable and unacceptable sample size, respectively.

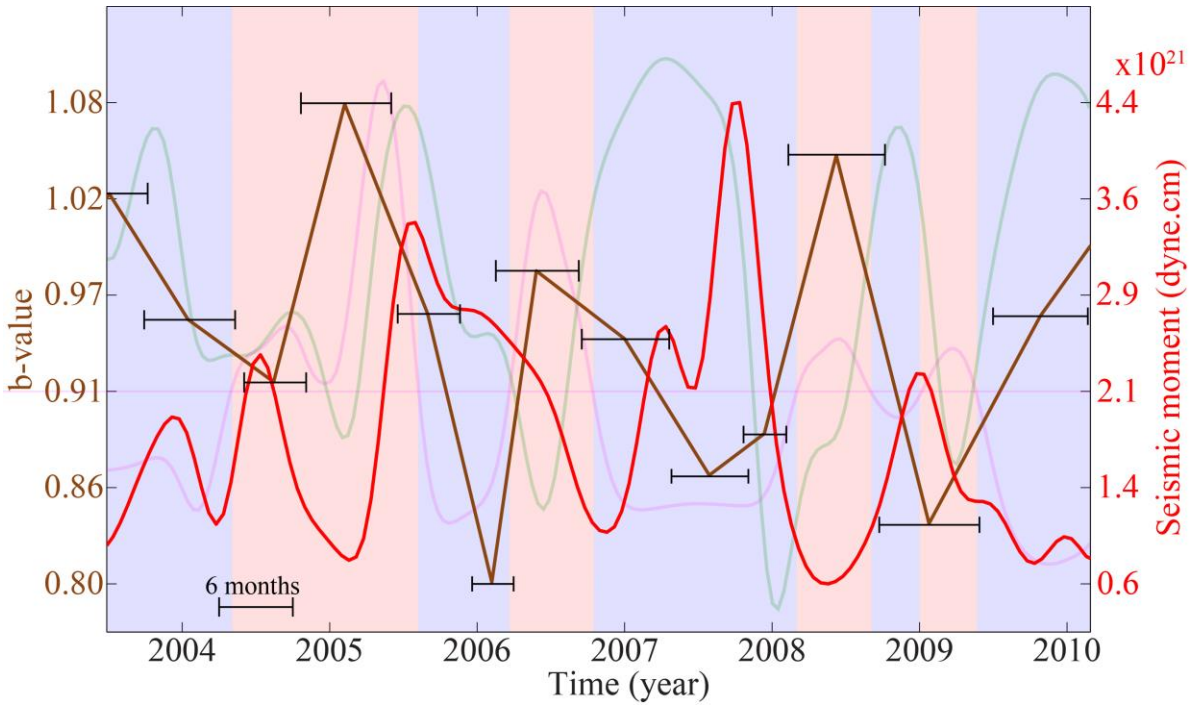

Supplementary Fig. 7| Time series of the released seismic moment (in red) calculated using moving temporal window of 3 months for the earthquake within 2 km distance from the central segment of the CSAF (from 20 to 90 km), versus the estimated *b*-value (in brown) considering M_c=1.3. The horizontal error bar on each estimated *b*-value shows the time interval encompassed by that estimation. A reference error bar with a length of 6 months is provided in the bottom left of the Figure. The magenta and green curves in the background respectively show the average rate difference and effective normal stress rate as shown in the Fig. 3 in main text. Beside the *b*-value, the other time series are smoothed using a Gaussian smoothing filter of size 6 months.

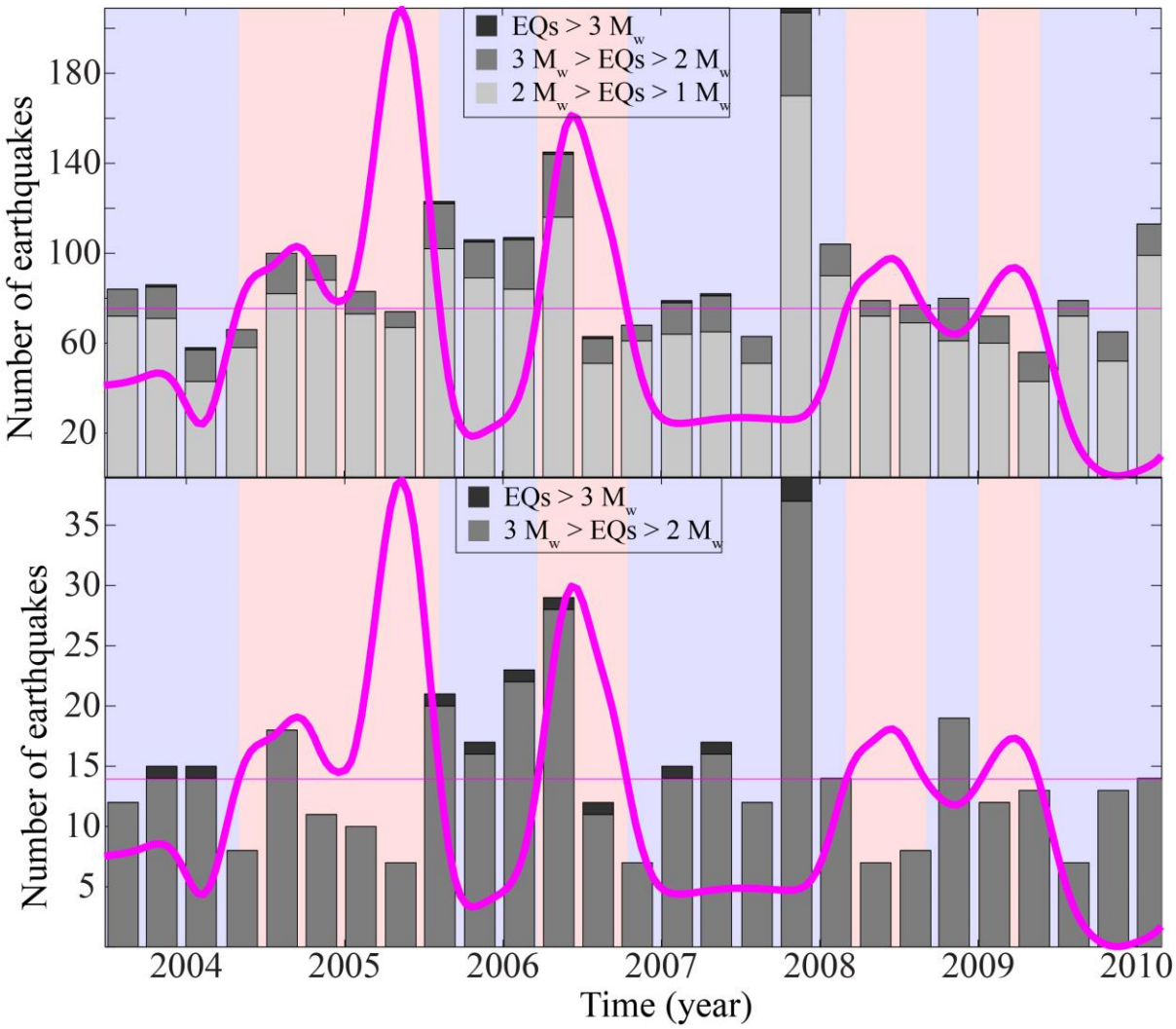

Supplementary Fig. 8| Time series of the number of earthquakes for the microseismicity within 2 km distance from the central segment of the CSAF (from 20 to 90 km). A temporal window of 3 months is used for this calculation. The magenta curve shows the average rate difference as shown in the Fig. 3 in main text. Top panel considers all the earthquakes larger than M_w1 with light gray showing the count for $M_w1.0 <$ EQs $< M_w2.0$, gray for $M_w2.0 <$ EQs $< M_w3.0$ and dark gray for $M_w3.0 <$ EQs. The bottom panel only considers earthquake larger than M_w2, with colors as defined above. No temporal smoothing is applied to the time series of earthquake count.

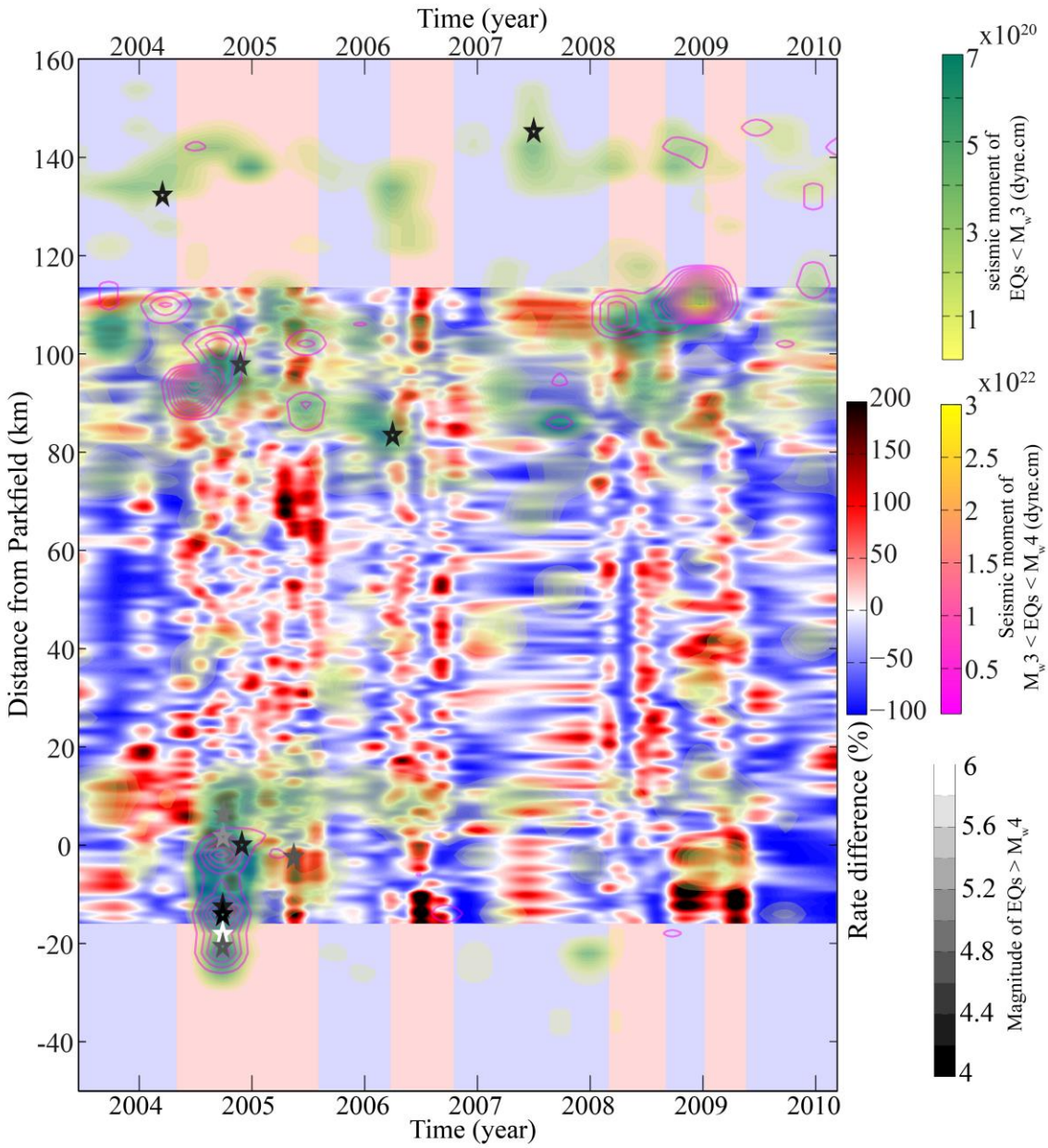

Supplementary Fig. 9| The same as Fig. 2 in the main text, but with detailed moment release map. Seismic moment released is shown using the contours in yellow to green colormap for EQs < M_w3, and in magenta to yellow colormap for M_w3 < EQs < M_w4. A moving window with spatial size of 6 km (step size of 4 km), and temporal size of 3 month is used to estimate the seismic moment for the earthquakes within 2 km of either side of the fault. Lastly, a Gaussian smoothing filter of size 6 months is applied in the temporal dimension.

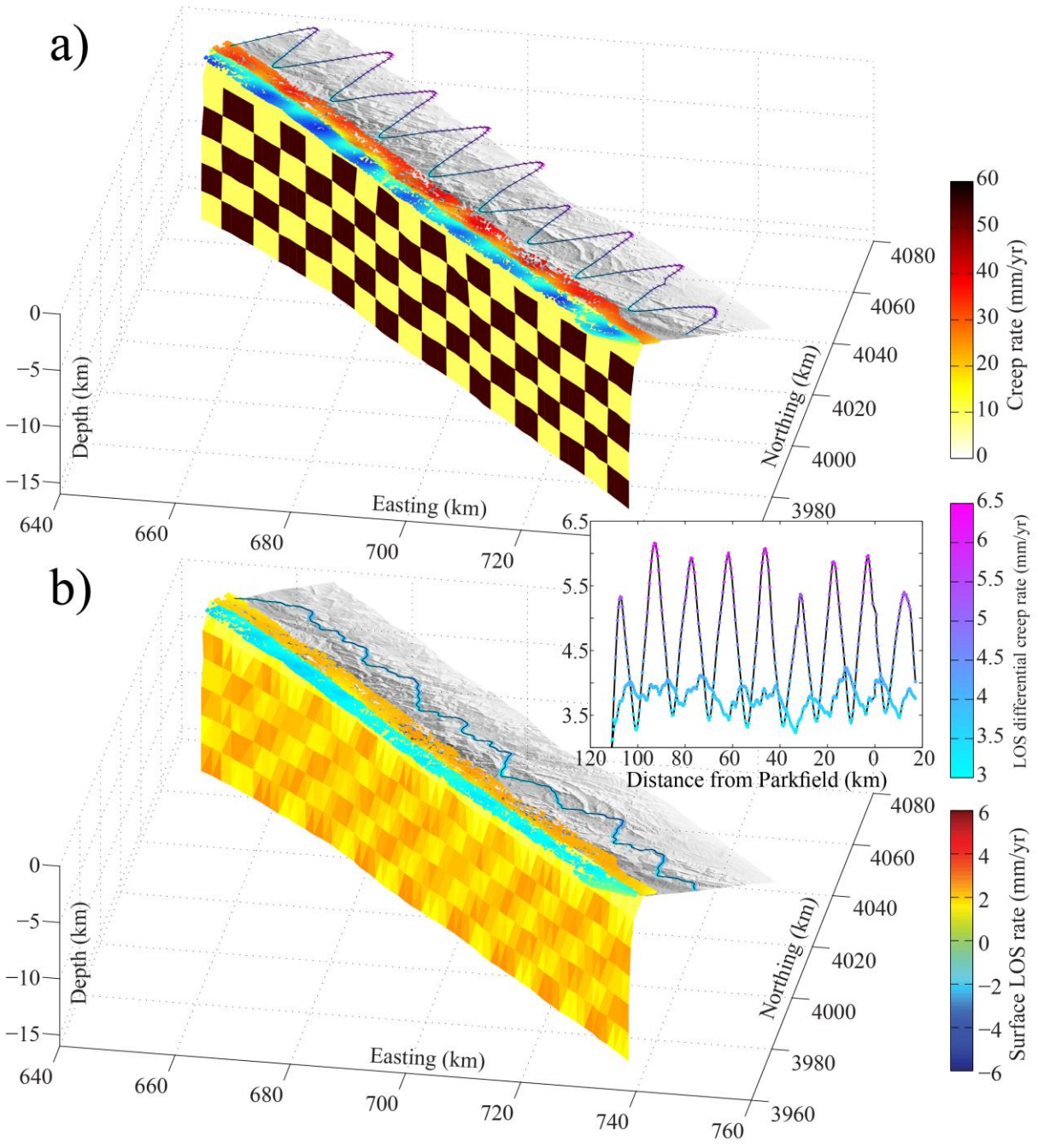

Supplementary Fig. 10| Modeled surface observation in LOS direction from two different scenarios for spatial distribution of creep rate (and pore pressure) along the CSAF. Creep rate on the fault is shown with color scale from yellow to black. Rainbow color scale is used for the LOS creep rate on the surface, estimated through forward modeling of the considered creep

distribution on the fault. The resulting near-distance LOS creep rate, estimated using the moving window (discussed in the main text) is also shown in the middle panel, using the color scale from cyan to magenta. **a**, Resulting from scenario #1 in which pore pressure is heterogeneously distributed within idealized rectangular compartments formed as a result of compaction of intergranular pore spaces. These compartments are considered to form in depths of more than 3 km. A 60 and 10 mm/yr creep rate, respectively, is considered for the high and low pore pressure compartments. **b**, Resulting from scenario #2, in which the porosity and permeability is increased due to accelerated creep events and pore pressure is more homogenously distributed within the fault. The creep rate in this scenario is considered to vary between 10 and 25 mm/yr across the fault, with relatively more homogeneous distribution compared to scenario #1. The middle panel compares the near-field LOS creep rate estimated from the two scenarios to emphasize the difference in the roughness of resulted profiles.